Journal of Hydrology 581 (2020) 124405

Contents lists available at ScienceDirect

Journal of Hydrology

journal homepage: www.elsevier.com/locate/jhydrol

Research papers

Improving remote sensing based evapotranspiration modelling in a heterogeneous urban environment

Mst Ilme Faridatul[a,b], Bo Wu[a,*], Xiaolin Zhu[a], Shuo Wang[a]

[a] Department of Land Surveying and Geo-Informatics, The Hong Kong Polytechnic University, Hong Kong
[b] Department of Urban and Regional Planning, Rajshahi University of Engineering & Technology, Bangladesh

ARTICLE INFO

This manuscript was handled by G. Syme, Editor-in-Chief, with the assistance of Shuo Wang, Associate Editor

Keywords:
Urban
Evapotranspiration
Remote sensing
Energy budget
Anthropogenic heat

ABSTRACT

Evapotranspiration (ET) is a key component of the hydrologic cycle. Knowledge of ET is important for modelling hydrologic fluxes and improving water resource management. Various remote sensing-based ET modelling studies have been conducted for investigating water demand in agricultural areas. However, ET modelling studies of urban areas are rare due to the challenges inherent in the heterogeneity of urban landscapes. This study proposes an improved surface energy balance algorithm for urban areas (uSEBAL) to make it suitable for estimating ET in urban environments. In the proposed approach, ET is predicted using improved energy budget components considering urban land cover composition and anthropogenic heat flux. The results of the uSEBAL are compared with the traditional method of SEBAL, and a sensitivity analysis is performed to evaluate the impact of uncertainties in ET estimates. The findings of this study indicate that the variability in urban land cover types impacts spatial variability in energy fluxes and ET. The results also show seasonal influence on ET for different land covers, but no significant influence of seasonality is observed on urban impervious areas, which produces the lowest ET nearly zero mm/day. The analysis of variance indicates that the differences between uSEBAL and SEBAL derived ET values for urban impervious areas are statistically significant (p-value < 0.05). The results also show the variability of ET values between models for other land cover types but show small variations in areas of wetland and dense vegetation. An investigation of factors of changes in ET indicates that surface albedo, and solar radiation highly influence ET, and the errors in the estimation of them can result in the highest uncertainty in the estimation of ET. The model performance metrics indicate that the uSEBAL is better than the SEBAL for estimating ET in a heterogeneous urban environment. This study supports the inclusion of anthropogenic heat in the energy budget, and emphasizes the use of land cover maps while estimate ET in urban areas.

1. Introduction

Evapotranspiration (ET) is a key component of the hydrologic cycle, which transfers from the earth surface to the atmosphere via evaporation and transpiration. ET links the terrestrial water and surface energy exchanges (Wang and Dickinson, 2012). It provides the atmospheric moisture that eventually returns to the earth in the form of rain and snow, and helps to cool the land surface temperature (Chen et al., 2014). In urban environment, land surface energy fluxes are known to vary, due in part to land cover heterogeneity (Weng et al., 2014). The diversity in urban land cover types and their changes influence the micrometeorological conditions and ET (Oke, 1979). Moreover, anthropogenic activities and unsustainable water management practices affect the hydrologic components, including ET. Sound knowledge of the spatial variations in ET is important for understanding the interactions between the atmosphere and the earth surfaces (Kustas and Norman, 1996; Chen et al., 2014), improving water resource management and predicting water usage under various geographical conditions (Wagle et al., 2017), and for investigating water stress and drought occurrence (McVicar and Jupp, 1998). Quantification of urban ET is also important for computing hydrologic fluxes e.g., recharge and runoff while using the water balance model (Trout and Ross, 2006).

Various ET estimation approaches have been developed and used to estimate the amount of water loss from geographical areas to the atmosphere (Magali et al., 2016; Wu, 2016; Wang et al., 2016). The techniques used to estimate ET can be commonly grouped as water balance approach, traditional estimation, empirical modelling, and remote sensing (RS) (Zhang et al., 2016; Kumar et al., 2018; Oberg and

* Corresponding author at: Department of Land Surveying and Geo-Informatics, The Hong Kong Polytechnic University, Hong Kong.
E-mail addresses: ilme.faridatul@connect.polyu.hk (M.I. Faridatul), bo.wu@polyu.edu.hk (B. Wu), Xiaolin.zhu@polyu.edu.hk (X. Zhu), shuo.s.wang@polyu.edu.hk (S. Wang).

https://doi.org/10.1016/j.jhydrol.2019.124405
Received 13 October 2019; Received in revised form 24 November 2019; Accepted 25 November 2019
Available online 29 November 2019

Melesss, 2006). The water balance approach is highly dependent on the availability of other hydrologic components and their accuracy (Scanlon et al., 2002). Traditional approaches (e.g. Bowen Ratio, Pan, Lysimeters, Eddy Correlation) provide an accurate estimation of ET, but are expensive and time-consuming; moreover, traditional approaches are limited to point data and therefore cannot provide ET estimates over large areas (Li and Zhao, 2010). Empirical models employ a numerical algorithm and input parameters that come from model calibration exercises and/or field investigations (Chen et al., 2007). Empirical models including the Makkink method (Makkink, 1957), Priestley-Taylor (Priestley and Taylor, 1972), Hargreaves-Samani (Jensen et al., 1990), and FAO Penman-Monteith (Allen et al., 1998) have been developed for modelling reference ET. However, none of these studies focused on ET estimation for a heterogeneous urban environment. In contrast, RS based approaches facilitate multi-temporal ET mapping on a regional scale and continuous monitoring of water loss to the atmosphere (Waters et al., 2002), making them a promising tool for monitoring and mapping ET for large areas (Bhattarai et al., 2016; Li and Zhao, 2010; Wagle et al., 2017; Bachour et al., 2014).

Five RS based ET models have been developed for predicting ET, including the surface energy balance algorithm for land (SEBAL) (Bastiaanssen et al., 1998), simplified surface energy balance index (S-SEBI) (Roerink et al., 2000), the surface energy balance system (SEBS) (Su, 2002), mapping ET at high resolution with internalized calibration (METRIC) (Allen et al., 2007), and the operational simplified surface energy balance model (SSEBop) (Senay et al., 2013). Various RS based studies have been conducted to estimate ET (El Garouani et al., 2000; Nouri et al., 2012; El Tahir et al., 2012; Xiong et al., 2010; Mutiga et al., 2010; Li and Zhao, 2010). Moreover, analyses have been conducted to evaluate and compare the performance of RS based ET models (Bhattarai et al., 2016; Wagle et al., 2017). To date, most of these previous studies focused on ET monitoring and mapping in agricultural areas for managing crop water demand.

Only a few studies have been conducted to estimate ET in an urban environment (Wang et al., 2016; Trout and Ross, 2006; Qiu et al., 2017; DiGiovanni-White et al., 2018; Grimmond and Oke, 1991). For example, Grimmond and Oke (1991) developed an urban ET model using an energy budget based on hourly measurements of micrometeorological flux. Their approach provided accurate hourly and daily estimates of latent heat and the state of surface water but the results were limited to point data. Trout and Ross (2006) introduced a method of predicting point measurement of ET using soil moisture data measured at various depths with capacitance sensors attached to a vertical probe. However, in addition to being expensive and labor-intensive, this approach cannot be used to obtain continuous data for vast areas without tremendous effort. Liu et al. (2010) used an ASCE reference ET algorithm and RS based evaporative fraction using land surface temperature (LST) and the mean temperature of hot and cold pixels to estimate urban ET. Wang et al. (2016) developed an empirical model to predict spatiotemporal patterns of urban ET in a subtropical desert climate for a metropolitan area. They used *in situ* flux measurement data from a local eddy tower and the LST and blue-sky albedo of moderate resolution imaging spectroradiometer (MODIS) land products. They developed a regression model to predict ET, and urged to use *in situ* ET measurements over various land cover classes.

Qiu et al. (2017) investigated the characteristics of ET in urban lawns and the factors that influence ET using the Bowen ratio, infrared RS, and three-temperature (3 T) model. They estimated ET of a fully covered vegetative lawn and assumed a reference leaf without transpiration in the 3 T model. However, in practice, it is not feasible to apply this model in areas that lack vegetation canopy, including the urban built environment. DiGiovanni-White et al. (2018) evaluated the influence of micrometeorological variability on the estimation of reference ET in a heterogeneous urban environment. They used Penman-Monteith based ASCE standardized reference ET algorithm to estimate ET at six weather stations using micrometeorological datasets. The study provided point data on predicted ET for six monitoring sites and urged to evaluate the influence of non-meteorological determinants such as soil type, vegetation type, moisture condition and anthropogenic heat flux on predictions of urban ET.

Although various ET modelling approaches are available (Bastiaanssen et al., 1998; Allen et al., 2007; Wu, 2016; Su, 2002), the estimation of ET for the heterogeneous urban environment is still a challenge (Wang et al., 2016; Trout and Ross, 2006; Qiu et al., 2017). This study aims to enhance existing RS based ET modelling in the typical urban environment using the principles of SEBAL developed by Bastiaanssen et al. (1998). The SEBAL is robust and has proved to be efficient in estimating ET in flat agricultural areas (Sun et al., 2011; Minacapilli et al., 2009; Jassas et al., 2015; Li and Zhao, 2010). The SEBAL was initially developed for predicting ET in agricultural areas, and thus a land cover (LC) map was not a requirement and overlooked anthropogenic heat in the energy budget, which is significant when analyzing urban environments. It is worth noting that LC map is useful for estimating the surface roughness parameters (Waters et al., 2002), and anthropogenic heat discharged from urban activities is one of the key components of urban energy budget (Wong et al., 2015; Oke, 1982); in the highly urbanized area, it should be included in the energy balance algorithm (Cong et al., 2017). Land surface parameters influence the exchange of energy among the atmosphere, hydrosphere and biosphere (Su, 2002) thus necessitate accurate estimation. This study aims to enhance the SEBAL so that it can map ET in a heterogeneous urban environment, and implement the resulting enhanced urban SEBAL (uSEBAL). In the proposed approach, the anthropogenic heat flux is delineated and included in the energy budget. Urban LC type is considered in delineating land surface parameters to allow reliable estimation of urban energy fluxes and improve ET mapping in a heterogeneous urban environment.

Section 2 includes a description of the study area and the experimental datasets, and describes improved algorithms of the energy budget components for ET modelling in urban areas. Section 3 details the experimental analysis, including a sensitivity analysis that is performed to assess uncertainties in the estimation of ET, and a model evaluation that involves a direct comparison of uSEBAL and SEBAL. Section 4 discusses the findings, and concluding remarks are presented in Section 5.

2. Materials and methods

2.1. Study area and experimental datasets

This study selects Dhaka, the capital city of Bangladesh as a research area, which is situated between latitudes 23.40° and 23.97° N and longitudes 90.20° and 90.59° E. For this study, an area of 604 km^2 covering Landsat Path 137 and Row 44 within zone 46 N is selected. The topography of the study area is relatively flat (Rahman et al., 2013) and its terrain mean elevation is 9.25 m (Fig. A.1). The study area is characterized by a humid subtropical monsoon climate. The mean annual precipitation is 2000 mm, with 80% occurring during the monsoon season. The temperature ranges from 28 °C to 34 °C in summer, from 26 °C to 30 °C in autumn, and from 10 °C to 21 °C in winter. Dhaka is one of the most densely populated megacities, with a population of nearly 18.23 million. Due to excess urbanization, the physical environment and water resources are changing and degrading the city's natural ecosystem (Islam et al., 2010).

Over the past decades, satellite images e.g., MODIS, Landsat, and Advanced Spaceborne Thermal Emission and Reflection Radiometer (ASTER) containing thermal bands have been commonly used to estimate ET. The spatial resolution of Landsat and ASTER is superior to MODIS images, and thereby favourable to small scale study. It should be noted that this study uses Landsat data because it offers a cross-calibrated medium resolution earth observation data of more than four decades, and thus allow for long-term multi-temporal analysis.

Table 1
List of datasets used in the analysis.

Date	Month	Year	Sensor	Season	Observed Pan Evaporation (mm/day)
10	Mar	2001	TM	Spring	6.5
13	Dec	2003	TM	Winter	3.3
02	Mar	2004	TM	Spring	5.0
15	Dec	2004	TM	Winter	3.7
25	April	2006	TM	Spring	5.6
19	Nov	2006	TM	Autumn	3.3
23	Feb	2007	TM	Spring	5.3
24	Nov	2008	TM	Autumn	2.7
28	Feb	2009	TM	Spring	5.0
27	Nov	2009	TM	Autumn	2.5
30	Jan	2010	TM	Winter	2.6
14	Nov	2010	TM	Autumn	2.1
06	Mar	2011	TM	Spring	5.5
07	April	2011	TM	Spring	6.0
06	Nov	2013	OLI	Autumn	2.4
24	Dec	2013	OLI	Winter	2.2

Moreover, Landsat data are publicly available and users are no longer restricted by precessing limitations (Markham and Helder, 2012; Wulder et al., 2016). Note that this study uses Landsat data however a future study is required to fully evaluate the applicability of this approach to other satellite data e.g., the ASTER.

It is important to use a totally clear sky cloud-free satellite images to estimate ET (Waters et al., 2002). This study uses 16 cloud-free Landsat images (Table 1) that are obtained from the US Geological Survey (https://earthexplorer.usgs.gov/). The spatial resolution of all the images is 30 m/pixel and the map projection is the Universal Transverse Mercator (UTM). It should be noted that this study uses images from 2001 to 2013 because corresponding *in situ* pan evaporation data which is used for validation are available on these dates. This study aims to estimate ET for every month and year from 2001 to 2013. However, the cloud-free Landsat images are rarely available to all of the months, years and seasons, thus this study uses 16 representative images of three seasons e.g., Spring (mid-February to April), Autumn (mid-August to November), and Winter (December to mid-February). In this study, the collected multi-year Landsat images are of level 1 thus image processing is carried out before computing the energy budget components. The solar incidence angle and atmospheric effects change the spectral properties of the images. Thus, radiometric and atmospheric corrections are applied to convert digital number values to surface reflectance. This study also uses meteorological data (e.g., wind speed, relative humidity, air temperature, atmospheric pressure, and pan evaporation) that are obtained from the Bangladesh Meteorological Department (BMD). It would be ideal to use meteorological data at the time that the satellite data were recorded but, due to the unavailability of data, this study uses the corresponding observed daily average meteorological data.

2.2. Improving surface energy budget components for ET modelling in urban areas

This study proposes an enhanced energy balance model to predict ET for heterogeneous urban environments. The satellite-based surface energy balance model is a parameterization of the energy fluxes, which requires few input parameters related to weather conditions. This study adopts the principles of the SEBAL and implements the proposed uSEBAL, which includes urban land surface parameters and considers anthropogenic heat flux. In this study, the atmospherically corrected Landsat images are classified using the support vector machine (SVM) algorithm. The classified land cover maps are used in the computation of surface energy budget components. The energy budget for the urban area is expressed as Eq. (1) (Oke, 1982). The SEBAL computes ET flux as shown in Eq. (2). In contrast, the proposed uSEBAL computes the ET flux as a residual of the urban energy budget, as shown in Eq. (3).

$$A + R_n = H + G_n + LE \quad (1)$$

$$LE = R_n - H - G_n \quad (2)$$

$$LE_U = A + R_n - H - G_n \quad (3)$$

where A, R_n, H, G_n, LE and LE_U represent urban anthropogenic heat, net radiation, sensible heat flux, net heat storage/soil heat flux, ET/latent heat flux and urban ET/latent heat flux in W/m^2 respectively.

The following sections describe the approach of improving and delineating energy budget components within Eq. (3). The algorithms are illustrated to compare and highlight the distinction between the SEBAL and proposed uSEBAL for improving ET modelling in urban areas.

2.2.1. Enhanced estimation of net radiation (R_n) in urban areas

Net radiation represents the actual radiant energy available at the surface, which is calculated by SEBAL as the sum of all of the incoming and outgoing radiant fluxes (Eq. (4)). The land surface parameters e.g. surface emissivity, albedo and LST are inputted to compute R_n. The SEBAL computes emissivity as a function of vegetation and leaf area index (Eq. (5)) (Waters et al., 2002).

$$\text{SEBAL}R_n = (1-\alpha)R_s\downarrow + R_L\downarrow - (\varepsilon_0\sigma\text{LST}) - (1-\varepsilon_0)R_L\downarrow \quad (4)$$

$$\varepsilon_0 = \begin{cases} 0.95 + 0.01LAI & where NDVI > 0 and LAI < 3 \\ 0.99 & NDVI < 0 \\ 0.98 & otherwise LAI \geq 3 \end{cases} \quad (5)$$

In contrast, the uSEBAL first assigns emissivity values to non-vegetative land cover (Van De Griend and Owe, 1993; Mallick et al., 2012) using the LC map and, then computes the emissivity of vegetative land as a function of vegetation index (Eq. (6)). The improved emissivity values are then inputted to delineate R_n (Eq. (7)).

$$\text{uSEBAL}\varepsilon_{0\_urban} = \begin{cases} water = 0.99;\ urbanimpervious = 0.95 \\ 1.0094 + 0.047 * \ln(NDVI) & for NDVI > 0.15 \\ 0.90 & otherwise \end{cases} \quad (6)$$

$$R_n = (1-\alpha)R_s\downarrow + R_L\downarrow - (\varepsilon_{0\text{urban}}\sigma\text{LST}) - (1-\varepsilon_{0\_urban})R_L\downarrow \quad (7)$$

where α is the surface albedo, $R_s\downarrow$ is the incoming shortwave radiation (W/m^2), $R_L\downarrow$ is the incoming long wave radiation (W/m^2), ε_0 is the surface emissivity, ε_{0_urban} is the emissivity of urban land surfaces, σ is the Stefan-Boltzmann constant, LST is the land surface temperature, LAI is the leaf area index and NDVI is the normalized difference vegetation index.

2.2.2. Enhanced estimation of soil heat flux (G_n) in urban areas

Soil heat flux is computed to estimate the rate of heat storage in the soil. The SEBAL approach uses Eq. (8) to estimate G_n in agricultural areas covered by vegetation. In uSEBAL, the LC map is considered to improve the estimation of G_n (Eq. (9)). Specifically, the proposed approach uses the algorithm from Bastiaanssen et al. (1998) to estimate G_n for vegetative land cover, and uses the coefficient values for water and urban areas as outlined in Kato and Yamaguchi (2005) to estimate G_n for urban non-vegetative land cover.

$$\text{SEBAL}G_n = R_n * \left(\frac{LST}{\alpha}(0.0038\alpha + 0.0074\alpha^2)(1 - 0.98NDVI^4)\right) \quad (8)$$

$$\text{uSEBAL}G_n = \begin{cases} R_n * \left(\frac{LST}{\alpha}(0.0038\alpha + 0.0074\alpha^2)(1 - 0.98NDVI^4)\right) & if land cover \\ & is\ vegetative \\ C_g * R_n & otherwise \end{cases} \quad (9)$$

where R_n is the net radiation (W/m^2), LST is the land surface temperature (°C), α is the surface albedo, NDVI is the normalized difference vegetation index and C_g is the coefficient of non-vegetative land cover.

2.2.3. Enhanced estimation of sensible heat flux (H) in urban areas

Sensible heat flux represents the rate of heat loss to the air due to the difference between surface and air temperatures. The SEBAL uses parameters including surface roughness (Z_{om}) as a function of LAI (Eq. (10)) and aerodynamic resistance to heat transport (r_{ah}) (Eq. (11)) to estimate H (Eq. (12)).

$$Z_{om} = 0.018 * LAI \tag{10}$$

$$r_{ah} = \frac{ln(z_2/z_1)}{k(\frac{0.4*u}{\ln(\frac{z_x}{z_{om}})})} \tag{11}$$

$$H = \rho C_p \frac{dT}{r_{ah}} \tag{12}$$

where LAI is the leaf area index, z_1 and z_2 are the heights in meters above the zero-plane displacement, k is von Karman's constant (0.4), u is the wind speed (m/s), z_x is the height of wind speed and air temperature, ρ is air density (Kg/m^3), C_p is the specific heat capacity of air (J/Kg/K), dT is the temperature difference and r_{ah} is the aerodynamic resistance to heat transport (s/m).

In the proposed uSEBAL model, the LC map is used to assign the values of Z_{om} for water, bare land and urban areas as outlined by Kato and Yamaguchi (2007) in addition to, Z_{om} values for vegetative land covers are estimated as a function of LAI. This study uses an algorithm developed by Verma (1989) to compute r_{ah} (Eq. (13)) for the uSEBAL because this algorithm has been widely used to estimate aerodynamic resistance to heat transport in urban environments, and has proved to be efficient in this type of application. Finally, the corresponding values of r_{ah} are used to delineate H (Eq. (12)).

$$r_{ah} = \frac{1}{ku*}\left[ln\left(\frac{z_x - d_0}{z_{0m}}\right) + ln\left(\frac{z_{om}}{z_{oh}}\right) - \psi H\right] \tag{13}$$

where d_0 is the zero-plane displacement height and ψH is the stability correction for heat, where ψ can be deemed as zero under neutral stratification.

2.2.4. Delineating anthropogenic heat flux (A) for impervious urban areas

The heat generated by human activities is referred to as anthropogenic heat, which comprises the heat discharged by the human metabolism, heating and cooling equipment, vehicle exhausts, commercial estates and industrial plants (Wong et al., 2015). In urban areas, human activities are concentrated in impervious areas, which generate anthropogenic heat. In contrast, the heat discharged from vegetation, water, and other natural land cover types is negligible. Thus, anthropogenic heat is assumed to be zero for non-impervious urban land covers.

To delineate urban anthropogenic heat, this study first computes the latent heat of impervious urban areas (LE_{imp}) using the algorithm from Wong et al. (2015). Second, net radiation of impervious urban areas (Rn_{imp}), the soil heat flux of impervious urban areas (G_{imp}) and the sensible heat flux of impervious urban areas (H_{imp}) are extracted from the energy fluxes (Eqs. (7), (9) and (12)) using the LC map. Lastly, Eq. (14) is used to compute urban anthropogenic heat for the entire area.

$$A = \begin{cases} G_{imp} + H_{imp} + LE_{imp} - Rn_{imp} if impervious urban cover \\ 0 otherwise \end{cases} \tag{14}$$

where G_{imp}, H_{imp} LE_{imp} and Rn_{imp} represent soil, sensible, latent heat and net radiation for impervious urban areas, respectively, in units of W/m^2.

2.2.5. Enhanced estimation of latent heat of vaporization (LE) and daily ET

Latent heat flux is expressed as the energy that accounts for the total water vapor that exchanges from the earth surface into the atmosphere (Rwasoka et al., 2011), and so represents the amount of heat loss from the earth surface due to ET (Waters et al., 2002). After computing LE (Eqs. (2) and (3)), the instantaneous evaporative fractions of the SEBAL and uSEBAL models are calculated using Eqs. (15) and (16). Lastly, 24-hour net radiation (R_{n24}) is computed following the procedure outlined in Allen et al. (1998) to estimate daily ET from the SEBAL and uSEBAL using Eqs. (17) and (18) respectively.

$$\Lambda = \frac{LE}{(R_n - G_n)} \tag{15}$$

$$\Lambda_{urban} = \frac{LE_u}{(R_n - G_n)} \tag{16}$$

where LE is the latent heat flux, R_n is the net radiation and G_n is the soil heat flux in W/m^2.

$$ET = \frac{86400}{\lambda \rho_w} \Lambda * R_{n24} \tag{17}$$

$$ET = \frac{86400}{\lambda \rho_w} \Lambda_{urban} * R_{n24} \tag{18}$$

where Λ is the evaporative fraction for the SEBAL, Λ_{urban} is the evaporative fraction for the uSEBAL, R_{n24} is the 24 h averaged net radiation in W/m^2, λ is the latent heat of vaporization in J/kg and ρ_w is the density of water in kg/m^3.

2.3. Model verification

This study proposes an approach to enhance the prediction of urban ET using the uSEBAL. To evaluate the results, first, a comparative analysis is performed between the predicted ET derived from the uSEBAL and the SEBAL. Second, model performance metrics e.g., coefficient of determination (R^2), mean absolute error (MAE), root mean square error (RMSE), and percent bias (PBias) are enumerated to verify the model. Finally, a sensitivity analysis is conducted to assess uncertainties in ET estimates.

To validate RS based ET, it is important to measure surface energy fluxes simultaneously for all land cover types at the time that the satellite overpass. However, this is a difficult task due to the technical and financial limitations. Moreover, *in situ* flux measurements are limited to point data, and thus the validation of large-scale energy fluxes and ET is not straightforward (Farah and Bastiaanssen, 2001). It is worth noting that the study area lacks a flux measurement tower. Therefore, model validation is conducted using *in situ* pan evaporation, which represents the amount of water loss from the earth surface to the atmosphere in the form of water vapor during a period (mm/day) with an unlimited supply of water (Sun et al., 2011). In this study, two different approaches are used to derive reference ET. First, reference ET is estimated using pan evaporation and pan coefficient values. This study computes pan coefficient using Eq. (19), and then enumerates reference ET using Eq. (20) (Allen and Pruitt, 1991). For further evaluation, reference crop ET is also computed based on the FAO Penman-Monteith algorithms (Allen et al., 1998).

$$K_p = 0.108 - 0.000331 * U_2 + 0.0422\, ln(Fetch) + 0.1434\, ln(RH_{mean}) - 0.000631[ln(Fetch)]^2 ln(RH_{mean}) \tag{19}$$

where U is the wind speed, and RH_{mean} is the average relative humidity.

$$ET_0 = K_p * E_{pan} \tag{20}$$

where K_p is the pan coefficient, and E_{pan} is the daily measured pan evaporation.

Finally, the reference ET is compared with predicted ET for evaluating the results of the proposed approach.

A sensitivity analysis is performed to evaluate the impact of uncertainties in ET estimates derived from the uSEBAL. This study applies a sensitivity analysis approach as proposed by Timmermans et al. (2007). They developed an algorithm for analyzing sensitivity to sensible heat flux, which is modified and applied in this study for assessing

the sensitivity to ET (Eq. (21)).

$$S_i = \left(\frac{ET_{\mp} - ET_0}{ET_0} \right) * 100\% \quad (21)$$

where S_i is the sensitivity of the model to an input i; ET_0, ET_- and ET_+ are the ET predicted by the model when the input energy flux equals its reference value i_0, and is decreased and increased respectively, with reference values used for all other inputs.

First, the reference input energy fluxes are obtained from the algorithms as described in Section 2.2. Second, the reference energy fluxes are averaged for six representative land cover types and predicted average ET_0 for each land cover type using Eq. (18). Third, the values of the input energy fluxes are perturbed to compute ET_- and ET_+, and the sensitivity to ET is enumerated. A deviation of 30 W/m^2 with a step of 5 W/m^2 is used to test the sensitivity of ET estimate.

3. Experimental analysis

In this section, first, a comparison is shown between surface energy fluxes of the uSEBAL and SEBAL. Second, the predicted ET that is derived using the uSEBAL is presented with an evaluation of the impact of spatial and temporal variations on ET. Then, these results are compared with the ET derived from the SEBAL. Lastly, the model performance metrics and sensitivity analysis results are briefly described.

3.1. Surface energy fluxes and spatial distribution of ET

Table A.1 summarizes the mean values of the predicted surface energy fluxes that are derived from the uSEBAL considering urban land cover types and anthropogenic heat, and the energy fluxes without considering them from the SEBAL. This study demonstrates an obvious difference in the estimation of surface energy fluxes, and these are variable to time and seasons. Fig. 1 presents the spatial distribution of land covers and daily ET. In this study, 16 images are used for predicting ET; however, to be concise, three representative land cover and ET maps of three seasons are presented in Fig. 1. In contrast, other maps are provided as supplementary material (Fig. A.2–4). In the ET maps, the lowest ET values are consistently observed in urban core areas dominated by impervious areas, which spread with increasing urbanization. In contrast, the highest ET values are found in areas of open water. Multi-year ET maps show gradual expansion of non-evaporative surfaces which indicate an increase in water scarcity, and thereby reduces overall ET in the urban area.

Table 2 and Table A.2–3 summarize the basic statistics of predicted ET for the different land cover types. The results demonstrate that ET values are variable to land cover classes and seasons. In the proposed approach, the highest ET values are again observed for open water and the lowest for urban impervious areas. Based on ET values, the land cover types are ranked in the order of open water > wetland/dense vegetation > sparse vegetation > sandy bare land > urban impervious. The results also indicate that ET increases in the Spring season and decreases in the Autumn and Winter season. During the Spring season, the highest ET values are observed for all of the land cover types. Note that the seasonal variations have influence on ET for different land cover types but no obvious influence is observed in the urban impervious areas. The results also indicate that ET values vary between Winter and Autumn season for different land cover types but the variations are very small. This study concludes that both land cover types and their changes, and seasonal variations have influence on ET.

3.2. Factors influencing changes in ET

To evaluate the factors influencing changes in ET, this study uses land surface parameters (e.g., surface albedo, LST, and NDVI) and weather parameters (e.g. solar radiation, wind speed, air temperature, and relative humidity). To investigate the interactions between predicted ET and the values of several important land surface parameters the coefficient of determination is computed for different land covers. Fig. 2 shows scatter plots of land surface parameters and predicted ET for two representative images. The results indicate a divergence in the relationship between land surface parameters and predicted ET for urban impervious areas. For further evaluation, the coefficient of determination for all of the non-impervious land covers are derived grouping them into one category as outlined in gray color.

It is evident that that open water has the lowest surface albedo and highest ET (Fig. 2(a) and (b)). In contrast, sandy bare land has the highest albedo and lowest ET among all the non-impervious land covers. In this study, wetlands seem to be covered by aquatic macrophytes. Thus, dense vegetation and wetland show very similar values for surface albedo and ET. The surface albedo of sparse vegetation is lower than that of bare land and higher than that of dense vegetation, thus ET of sparse vegetation is higher than that of bare land and lower than that of dense vegetation. Importantly, it is noted that surface albedo shows a strong negative correlation with ET for non-impervious land cover. In contrast, impervious urban areas show surface albedo values similar to sparse vegetation but ET was close to zero, showing divergence in the relationship between ET and surface albedo in impervious urban areas. A strong coefficient of determination (R^2 = 0.93 and 0.96) between ET and surface albedo was observed for the non-impervious land cover types.

Scatter plots of LST and predicted ET by land cover type show that open water has the lowest LST and highest ET (Fig. 2(c) and (d)). In contrast, sandy bare land has the highest LST and lowest ET among all the non-impervious land covers. It is also notable that impervious areas show divergence in ET and LST form other non-impervious land covers. These results indicate that LST can explain the variation in ET for different land cover types except for impervious urban areas. The coefficient of determination between LST and non-impervious land cover is nearly 0.85.

Fig. 2(e) and (f) shows the coefficient of determination between NDVI and ET. The results indicate that homogeneous areas covered by sparse and dense vegetation canopy to some extent explain the observed variation between NDVI and ET. However, NDVI cannot be used to explain the spatial variation in ET for a heterogeneous urban environment.

The scatter plots of land surface parameters demonstrate that surface albedo and, to a lesser extent, LST highly influence ET. However, urban impervious areas show divergence in the distribution of ET. In addition, the wetlands also deviate to some extent because LST, precipitation, and growth of aquatic macrophytes bring changes in the characteristics of wetland areas (Jiang et al., 2017). The investigations confirm that urban landscapes are diverse thus ET prediction in the heterogeneous environment is not straightforward, and care should be taken to map ET in urban areas.

To evaluate temporal variation in ET, this study computes the correlation between mean predicted ET and corresponding daily average relative humidity, wind speed, air temperature and solar radiation (Fig. 3). The results indicate that variation in solar radiation shows the highest coefficient of determination for change in ET (Fig. 3(d)), followed by variation in air temperature (Fig. 3(b)). This finding corroborates analysis by Qiu et al. (2017) that ET is strongly correlated with solar radiation in urban areas.

Note that micrometeorological variability can influence reference ET in a heterogeneous urban environment (DiGiovanni-White et al., 2018). The wind speed, as well as solar radiation, can affect ET (McVicar et al., 2012); however, the results of this study show little influence of wind speed and relative humidity on ET. It is worth noting that this study uses meteorological datasets from only one weather station, which is located in the core of the study site. Weather datasets from different locations will be used in future work to further investigate the influence of meteorological parameters on the variation in

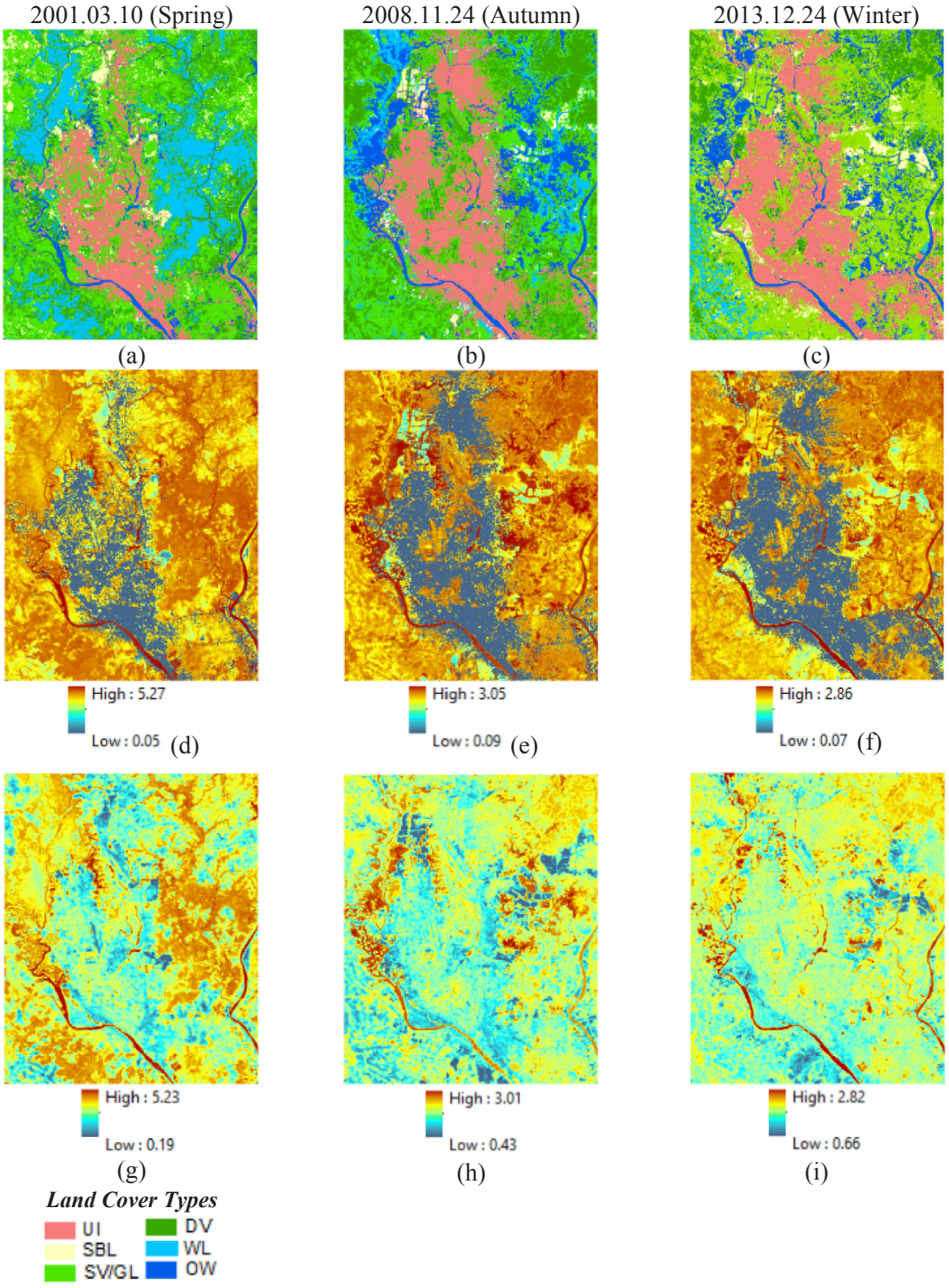

Fig. 1. Spatial distribution of land cover types (a)–(c), and daily ET derived from the (d)–(f) uSEBAL, and (g)–(i) SEBAL. Note: OW, open water; WL, wetlands; DV, dense vegetation; SV, sparse vegetation; SBL, sandy bare land and UI, urban impervious.

ET.

The analysis confirms that surface albedo, LST, solar radiation and air temperature strongly influence ET compared to other parameters. However, impervious urban areas show a high level of variability in the characteristics of the land surface parameters, and thus care should be taken to map ET in urban environments.

3.3. Comparison analysis and performance evaluation

3.3.1. Comparison of predicted ET

In this study, ET is predicted for 16 datasets using the uSEBAL and SEBAL. However, to be concise, the comparative analysis is presented in detail for three datasets. The results from the SEBAL and the histogram distribution for other datasets are provided as supplementary material (Fig. A.5–6).

Fig. 4 presents the delineated histograms and local spatial difference between ET derived from the uSEBAL and SEBAL for the dataset of

Table 2
Basic statistics of predicted ET (mm/day) for different land cover types.

Model	Date	Basic Statistics	Land Cover Types						
			OW	WL	DV	SV	SBL	UI	Overall
uSEBAL	2001.03.10 (Spring)	Max	5.27	4.72	4.97	4.60	2.87	0.35	5.27
		Min	3.79	2.84	2.05	0.21	0.04	0.02	0.02
		Mean	4.82	4.18	4.21	3.62	1.86	0.25	3.36
	2008.11.24 (Autumn)	Max	3.05	2.72	2.72	2.57	2.12	0.11	3.05
		Min	2.42	1.00	1.92	0.10	0.09	0.09	0.08
		Mean	2.80	2.19	2.45	1.96	1.46	0.10	1.83
	2013.12.24 (Winter)	Max	2.85	2.35	2.54	2.59	2.09	0.11	2.85
		Min	2.00	1.60	1.98	0.11	0.09	0.08	0.08
		Mean	2.58	2.08	2.32	2.05	1.39	0.10	1.61
SEBAL	2001.03.10 (Spring)	Max	5.23	4.75	4.92	4.65	3.00	4.80	5.23
		Min	2.56	2.10	2.18	1.39	0.19	0.41	0.19
		Mean	4.52	4.14	4.02	3.44	2.65	3.21	3.65
	2008.11.24 (Autumn)	Max	3.01	3.01	2.72	2.99	2.21	2.61	3.01
		Min	2.08	1.23	1.62	0.43	0.40	1.29	0.40
		Mean	2.67	2.25	2.35	2.17	1.47	2.12	2.25
	2013.12.24 (Winter)	Max	2.81	2.26	2.52	2.42	2.18	2.60	2.81
		Min	1.98	1.47	1.85	1.09	0.66	1.12	0.66
		Mean	2.45	1.97	2.25	2.04	1.62	2.01	2.07

2001, 2008 and 2013. The central part of the study area is dominated by impervious urban areas; therefore, ET is low in the city centre compared to the fringe areas. The uSEBAL produces the lowest ET values for impervious urban areas, followed by sandy bare land (Fig. 1(d)–(f)). In contrast, the SEBAL produces the lowest ET values for sandy bare land followed by impervious areas (Fig. 1(g)–(i)). The histogram distribution of ET (Fig. 4(a)–(c)) illustrates that the uSEBAL produces an ET value of nearly zero for more than 100 000 pixels. In contrast, the SEBAL shows an insignificant number of pixels with an ET of nearly zero (Fig. 4(d)–(f)). The results of the other datasets (Fig. A.5) show similar findings to those for the dataset from 2001, 2008 and 2013.

Fig. 5 presents the local spatial difference between ET derived from the uSEBAL and SEBAL. The impervious areas show strong deviations between the results of uSEBAL and SEBAL in the prediction of ET for the dataset of 2001 (Fig. 5(a)). In contrast, vegetative land covers and open water areas show low deviations in ET between the models. The deviations in the estimated ET in the 2008 and 2013 dataset (Fig. 5(b) and (c)) and other datasets (Fig. A.6) show similar findings to those for the dataset of 2001.

Table 2 shows the differences in basic statistics of predicted ET derived from the uSEBAL and SEBAL for three datasets. This study also computes basic statistics of other datasets for both models, which are provided as supplementary material in Table A.2–3. The comparison analysis indicates the differences between uSEBAL and SEBAL derived ET values for different land cover types. However, the overall maximum predicted ET values are nearly similar in both models. In contrast, a large variation is observed in the minimum and mean ET values. In this study, the analysis of variance (ANOVA) is used to test the significance of the differences between uSEBAL and SEBAL derived ET. The results of ANOVA as shown in Table 3 indicate that the differences between overall minimum and mean ET values are statistically significant (p-value < 0.05). The result also indicates that the differences between uSEBAL and SEBAL derived minimum, maximum and mean ET values for urban impervious areas are statistically significant (p-value < 0.05). The differences in mean ET values for open water and sandy bare land, the differences in maximum ET values for sparse vegetation and sandy bare land are also statistically significant (p-value < 0.05). Note that wetland and dense vegetation show differences between uSEBAL and SEBAL derived ET values but their differences are not significant. In summary, the results indicate that the predicted ET values vary between two models but all the variations are not statistically significant. The uSEBAL yields the lowest ET values for a large number of pixels that contained impervious areas (Fig. 4(a)–(c)). Thus, the overall mean ET values are lower in the uSEBAL than in the SEBAL.

3.3.2. Model performance

To verify the models, the predicted mean evaporation for the bodies of surface water is delineated from 16 ET maps, and then the regression analysis is performed against the measured pan evaporation (Fig. 6(a) and (b)). The uSEBAL show a strong coefficient of determination ($R^2 = 0.84$) compared to the SEBAL ($R^2 = 0.77$). The uSEBAL also indicate better performance than the SEBAL in terms of RMSE, MAE, and PBias.

For further evaluation, using Eq. (20) reference ET is estimated based on pan evaporation data and used as the measured ET to establish the relationship between ET derived from the SEBAL and uSEBAL. Overall, the uSEBAL has a higher coefficient of determination ($R^2 = 0.79$) than the SEBAL ($R^2 = 0.74$) (Fig. 6(c) and (d)). In addition, the RMSE, MAE and PBias values of the uSEBAL are better than those of the SEBAL. Fig. 6(e) and (f) show the coefficient of determination between predicted and reference ET derived from FAO Penman-Monteith algorithm. This evaluation also shows that the uSEBAL yields a higher coefficient of determination ($R^2 = 0.78$) than the SEBAL ($R^2 = 0.74$). However, the variations in the other model performance metrics are not significant.

3.3.3. Model sensitivity

In the results of a sensitivity analysis using two representative datasets, Fig. 7(a) and (b) show that R_n is positively correlated with ET. A 30 W/m^2 increase and decrease in R_n result in the highest change in the estimate of ET for sandy bare land and impervious urban areas, followed by sparse vegetation. In contrast, the changes in R_n for other land cover types show no significant sensitivity to ET. A linear negative correlation between G_n and ET (Fig. 7(c) and (d)) shows that an increase in G_n cloud led to a decrease in ET; however, sandy bare land and urban impervious areas are highly sensitive compared to other land cover types. A 30 W/m^2 increase and decrease in G_n results in around an 8% change in ET. Changes to H are negatively correlated with ET and the correlations are approximately linear (Fig. 7(e) and (f)). A 30 W/m^2 increase and decrease in H results in the highest relative change in ET of around 25–30% for impervious urban areas, followed by 15% changes in ET for sandy bare land. Note that the changes in H are highly sensitive to ET compared to the changes in R_n and G_n. Fig. 7(g) and (h) show that the changes in LE are positively correlated with ET. A 30 W/m^2 increase and decrease in LE results in a more than

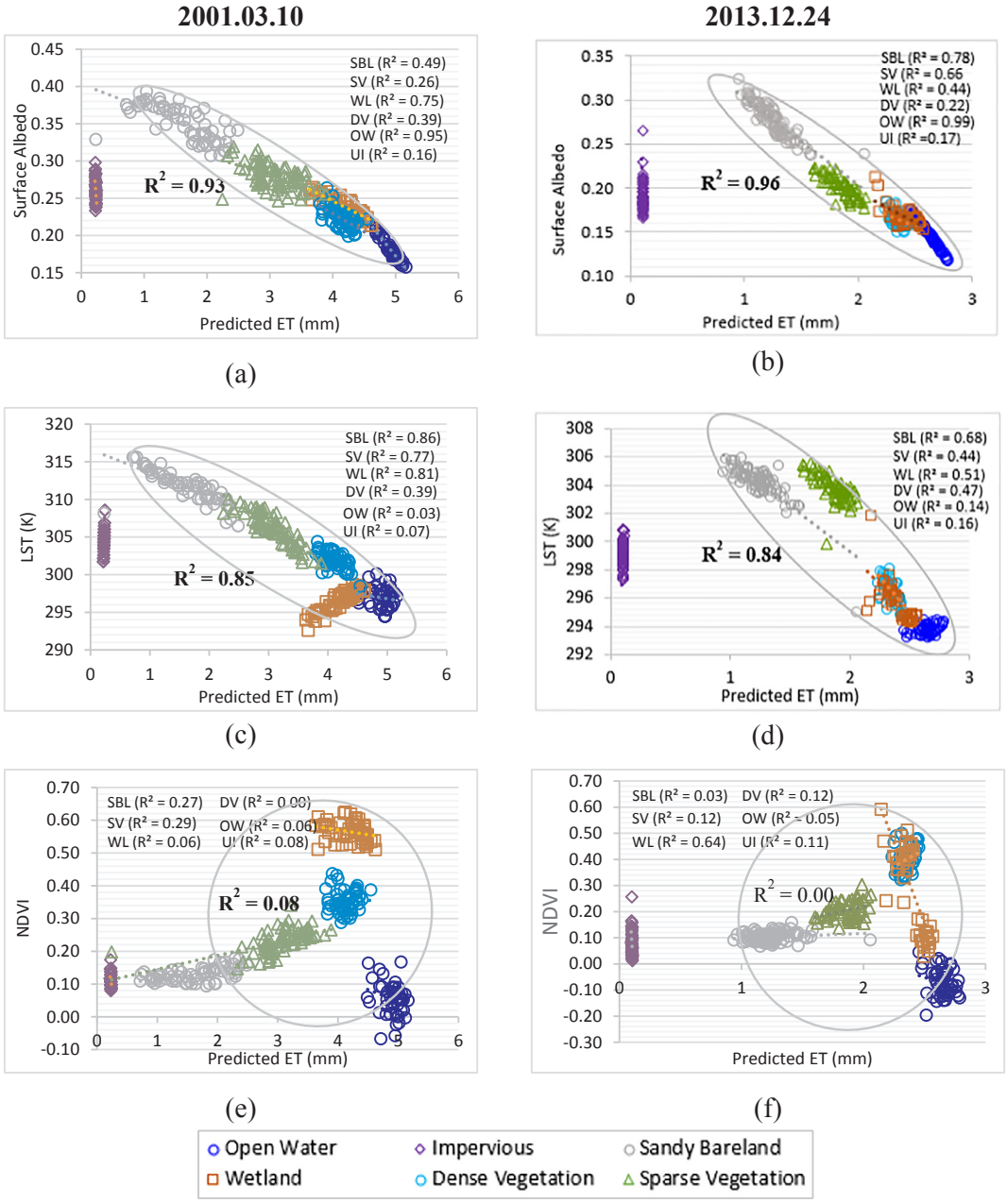

Fig. 2. Scatter plots of land surface parameters and predicted ET: (a),(b) surface albedo and predicted ET, (c),(d) LST and predicted ET, and (e),(f) NDVI and predicted ET.

20% change in the estimation of ET for impervious urban areas. Note that the change in LE for other land cover types is also sensitive to ET but shows a lower relative change than that for impervious urban areas.

The results of sensitivity analysis indicate that the errors in input energy fluxes can result in an inaccurate estimation of ET. However, sensitivity is variable to energy fluxes and land cover types. The results demonstrate that the model is most sensitive to changes in LE and H followed by R_n and G_n. Note that dense and sparse vegetation are less sensitive to changes in ET than other land cover types.

It should also be noted that the errors in input parameters can result in an inaccurate estimation of the energy budget components. This study investigates model sensitivity to changes in input parameters, including LST and surface albedo that is derived from Landsat images; air temperature and solar radiation that is collected from the weather station. Among various factors of changes in ET, this study finds a high influence of these four parameters. The values of input parameters are perturbed and the sensitivity to energy budget components is enumerated. Fig. 8 shows an example of sensitivity to changes in surface albedo, LST and air temperature for sandy bare land in the estimation of surface energy fluxes. The results of sensitivity analysis for other land cover types are provided as supplementary material (Fig. A.7–9). The results demonstrate that surface albedo is highly correlated with LE followed by R_n. A 12.5% increase and decrease in surface albedo result in the highest change in the estimation of LE. In contrast, an increase and decrease in LST and air temperature show the highest change in the estimation of LE followed by H for sandy bare land and urban impervious areas. In contrast, other land cover types show the highest change in the estimation of H followed by LE. A 5 K increase and decrease in surface and air temperature results in a more than 40% change in the estimation of LE, and nearly 30% change in the estimation of H.

As mentioned previously, solar radiation strongly influences ET thus Fig. 7(i) and (j) indicates that the change in 24-hour net radiation is

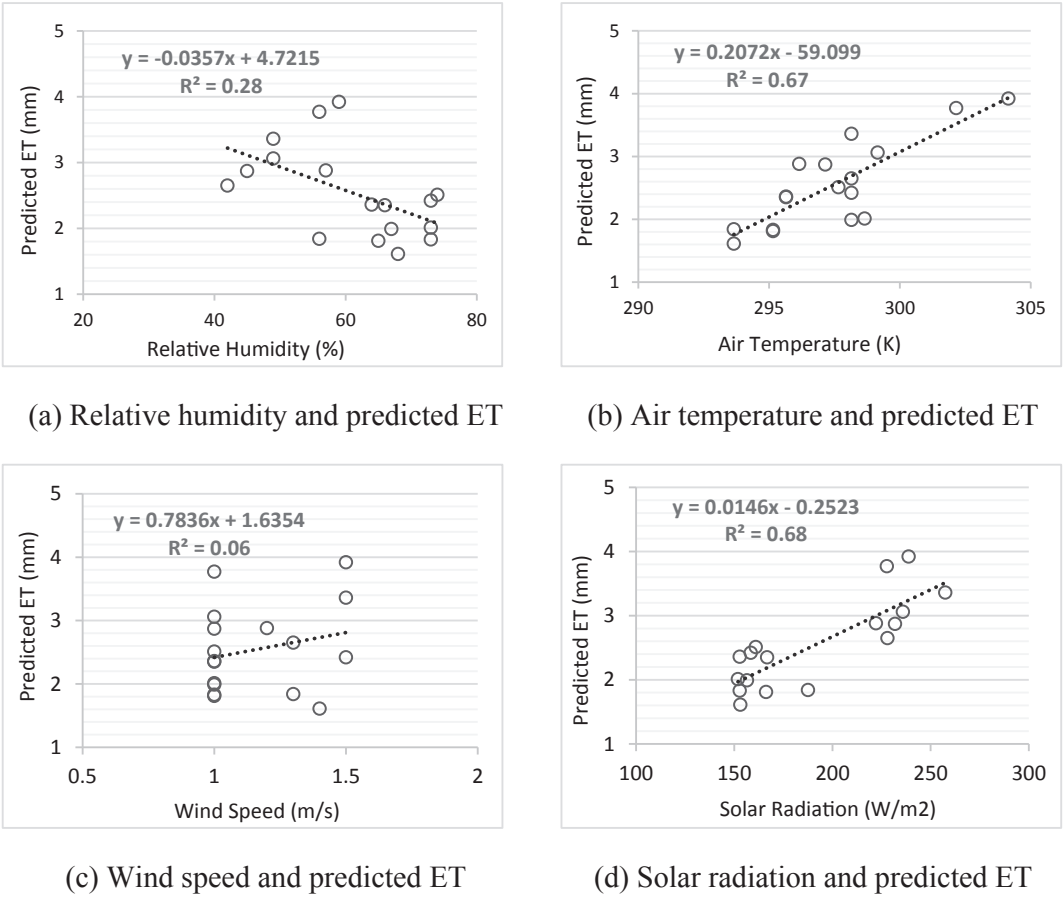

Fig. 3. Coefficient of determination between weather parameters and ET.

highly sensitive to ET. It shows a positive and linear correlation with ET. A 30 W/m^2 increase and decrease in R_{n24} results in a more than 20% change in the estimation of ET.

The sensitivity analysis results demonstrate that impervious urban areas and sandy bare lands are highly sensitive to changes in energy budget components compared to other land cover types. Thus, care should be taken in the estimation of surface energy fluxes for ET modelling in the typical urban areas.

4. Discussion

The findings of this study suggest using a land cover map for the estimation of ET in the urban environment because urban land cover types are diverse in nature, and the variability in land cover types impacts spatial variability in energy fluxes and ET. Waters et al. (2002) mentioned that land cover map is not a requirement for surface energy balance algorithm but is highly recommended. The existence of large impervious surfaces makes ET estimation a challenge in urban areas (Trout and Ross, 2006). This study acknowledges the consideration of urban land cover classes to estimate urban energy fluxes. The uSEBAL with consideration of urban land cover types shows variation in the estimation of energy fluxes from the traditional SEBAL (Table A.1). The estimated net radiation shows the lowest difference between SEBAL and uSEBAL. In contrast, other energy fluxes e.g., soil heat flux, sensible heat flux, and latent heat flux show the largest variation between them. The results show variability in the predicted energy fluxes to dates.

It is important to validate predicted energy fluxes however, this study lacks *in situ* measurement thus future work is a requirement. This study evaluates the estimated energy fluxes, by comparison, the results of some other studies. In an analysis of intra-urban energy fluxes, Weng et al. (2014) found the ranges of net radiation from 319 to 613 W/m^2, soil heat flux from 97 to 176 W/m^2, sensible heat flux from 93 to 165, and latent heat flux from 96 to 195 W/m^2. The results of the uSEBAL show more consistency in the estimation of net radiation and soil heat flux than the SEBAL. The sensible heat flux of some dates shows relatively low values while using the uSEBAL; in contrast, the SEBAL yields relatively low values for all of the dates. In the proposed approach, the mean values of the latent heat flux show overestimation but relatively low than the mean values as derived using the SEBAL. The deviations in the estimation of the energy fluxes can arise due to the variation in geographical settings and weather conditions. However, the observation of this study is consistent with findings reported in an analysis of Weng et al. (2014) that urban energy fluxes are variable to dates and seasons.

The characteristics of the physical properties and diverse landscapes affect land surface parameters in urban environments. Multi-year image analysis indicates that the spatial variation in land cover and seasons strongly influence ET. The values of the land surface parameters and predicted ET are also characterized by spatial and temporal variation of the landscapes. Land surface parameters (e.g., surface albedo and LST) show a strong negative correlation with ET for non-impervious land cover types. The spatial distribution of ET generally follows the spatial variation in surface temperature (Bhattarai et al., 2016). However, this study shows that ET is strongly correlated to LST in non-impervious areas, but show greater deviation in areas containing impervious land cover.

This study supports the inclusion of anthropogenic heat in the energy budget while estimate ET in an urban environment using the principles of land surface energy balance. The results of this study indicate that the inclusion of anthropogenic heat and consideration of urban land cover composition improves ET estimation in a heterogeneous urban environment and facilitates to map ET in urban areas. As

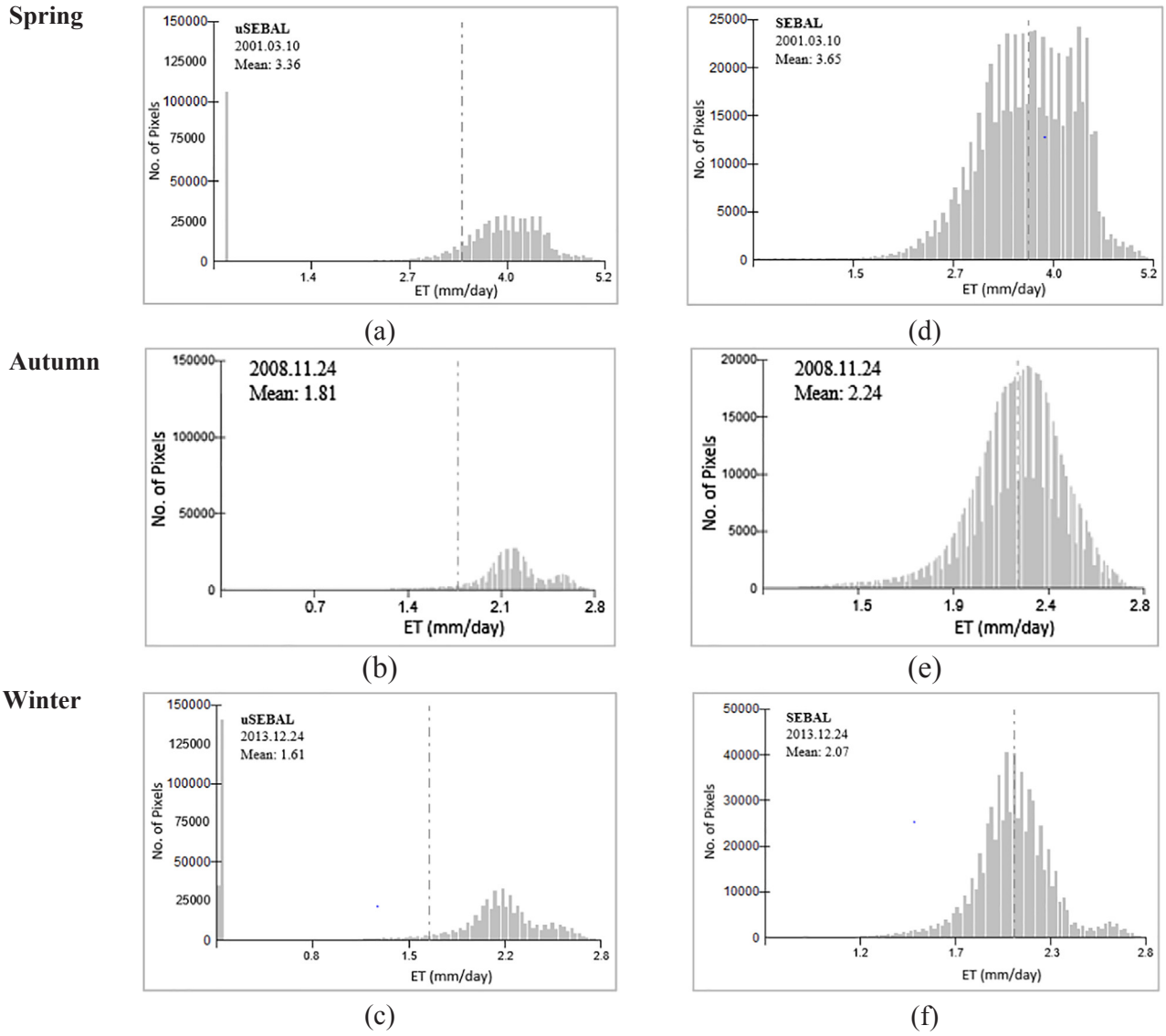

Fig. 4. Comparison of predicted ET: (a)–(c) histograms derived from the uSEBAL and (d)–(f) histograms derived from the SEBAL.

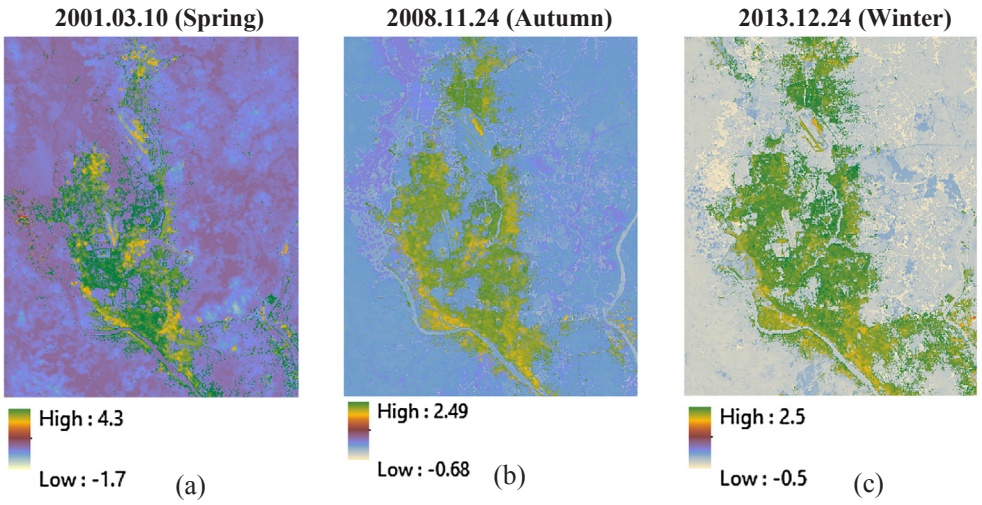

Fig. 5. Local spatial difference of predicted ET between uSEBAL and SEBAL.

Table 3
Statistical significance of the differences between uSEBAL and SEBAL derived ET.

Statistics	OW	WL	DV	SV	SBL	UI	Overall
Max	0.95	0.71	0.91	0.05*	0.02*	0.00*	0.95
Min	0.86	0.22	0.41	0.003*	0.79	0.00*	0.00*
Mean	0.04*	0.70	0.87	0.36	0.02*	0.00*	0.04*

Note: *p-value is statistically significant at the 0.05 level.

mentioned previously, the comparative analyses show significant deviations in the predicted ET for impervious urban areas. This corroborates previous studies showing that impervious urban areas are non-evaporative and that ET is generally small in areas with no water (Ma et al., 2013) because dry areas generate the lowest latent heat flux (Farah and Bastiaanssen, 2001). A substantial variation in latent heat of vaporization for impervious urban areas is evident between SEBAL and uSEBAL. The proposed approach provides the lowest latent heat for impervious urban areas (Fig. 9). Therefore, the uSEBAL results in the lowest ET for the impervious urban areas. In contrast, the SEBAL overestimate ET for impervious urban areas. Note that Kato and Yamaguchi (2007) reported zero LE for urban areas. In addition, Wong et al. (2015) reported that latent heat in urban areas is very low (around 5 to 10 W/m^2). The findings of this study show good agreement with the findings of Kato and Yamaguchi (2007) and Wong et al. (2015). Impervious areas are the dominant land cover in urban environments and anthropogenic heat is a significant energy flux. Thus, it is important to consider this heat flux in the energy balance algorithm.

It should be noted that various meteorological parameters, including solar radiation, relative humidity, air temperature, and wind speed affect ET (Shi et al., 2017; Tabari et al., 2012; Tomer and Schilling, 2009). However, the most important factor influencing ET is not stationary. Du et al. (2016) indicated relative humidity as the factor most sensitive to seasonal and annual changes in ET in the Heihe river basin of northwestern China. McVicar et al. (2012) found wind speed as the dominant force of changes in ET. Tabari et al. (2012) indicated that

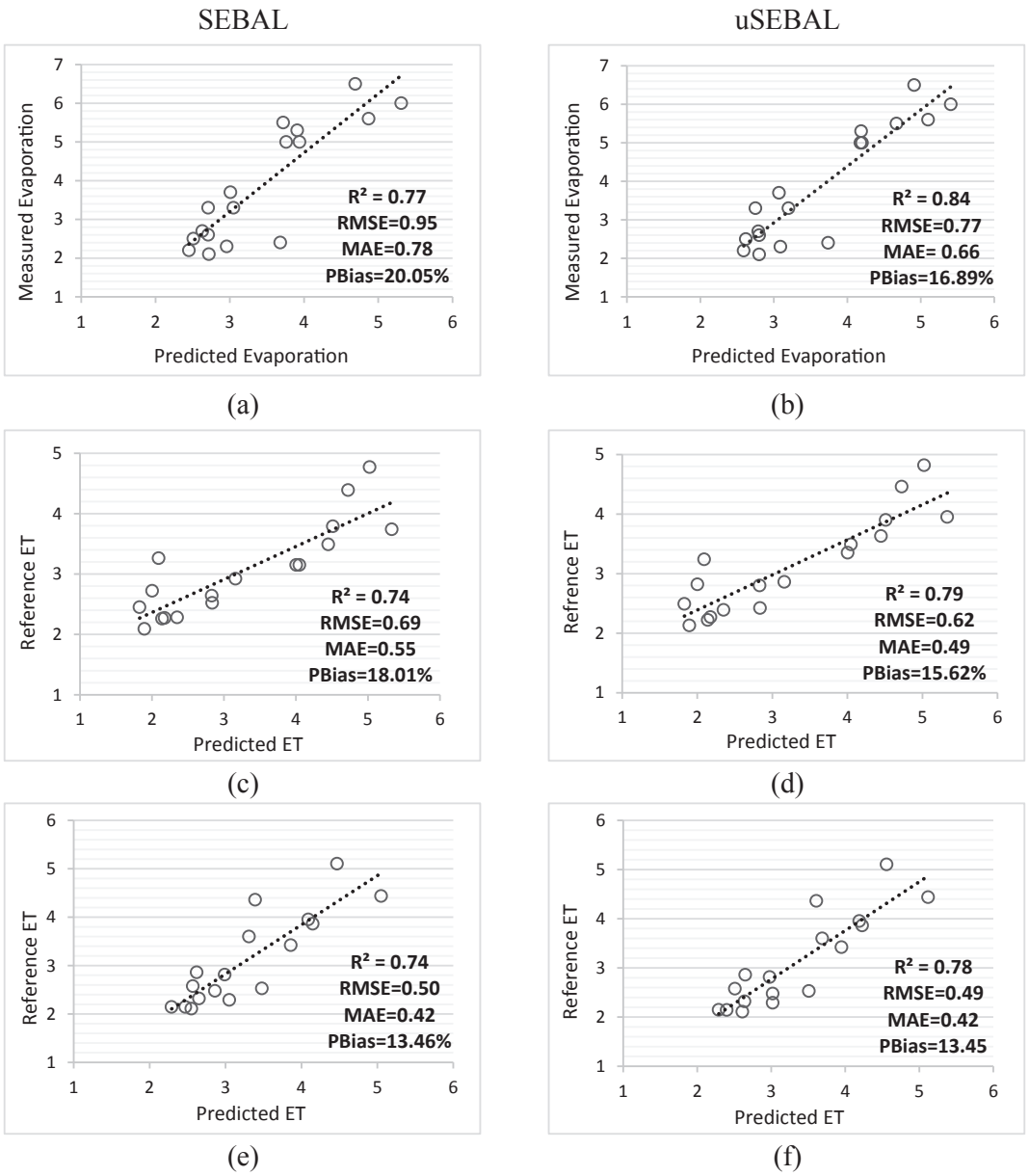

Fig. 6. Comparison of regression plots and model performance statistics: (a),(b) measured pan evaporation vs. predicted evaporation from open water, (c),(d) reference ET derived from pan evaporation vs. predicted ET, and (e),(f) reference ET derived from FAO Penman-Monteith vs. predicted ET.

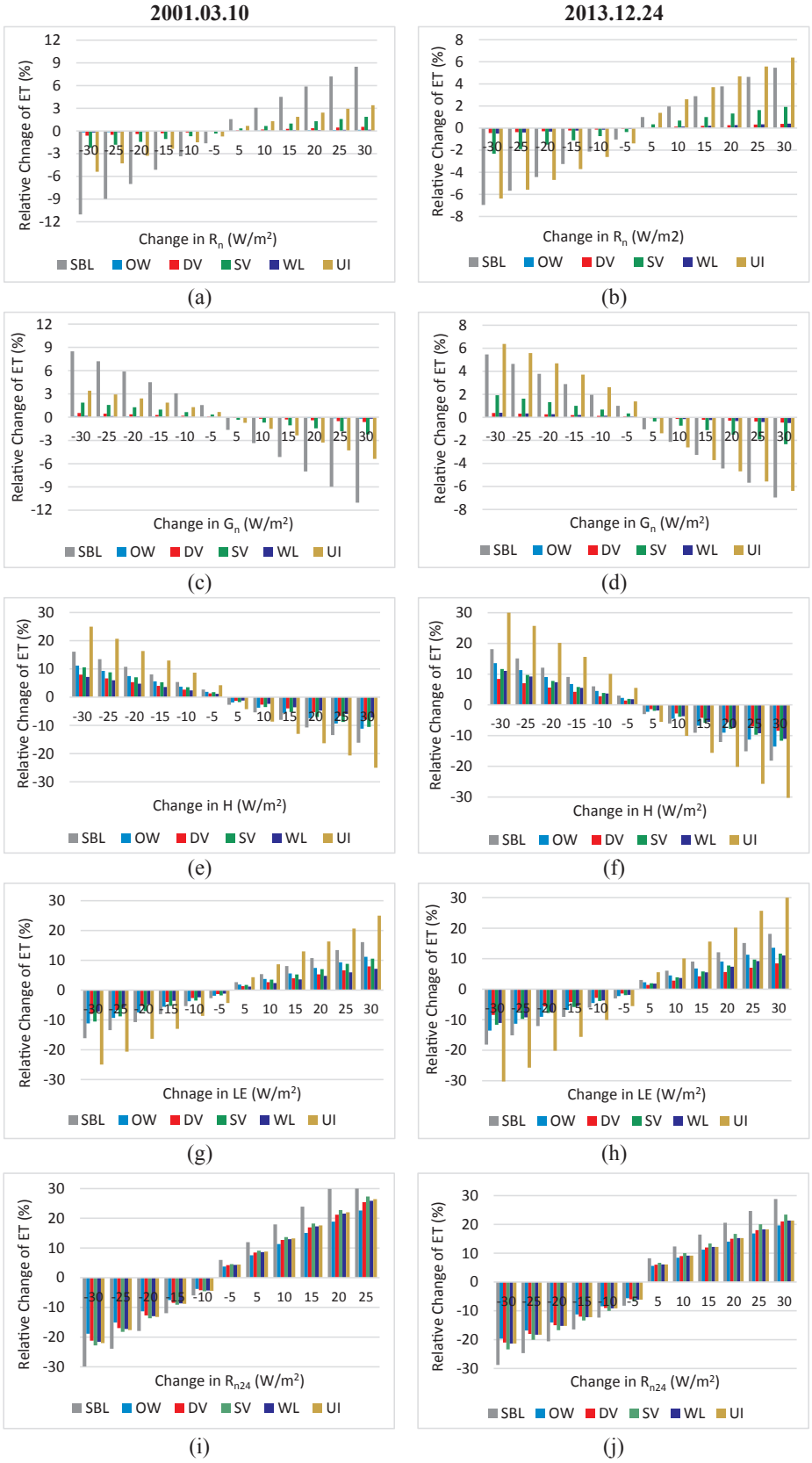

Fig. 7. Sensitivity of ET to changes of the energy budget components: (a),(b) change in R_n, (c),(d) change in G_n, (e),(f) change in H, (g),(h) change in LE, and (i),(j) change in R_{n24}.

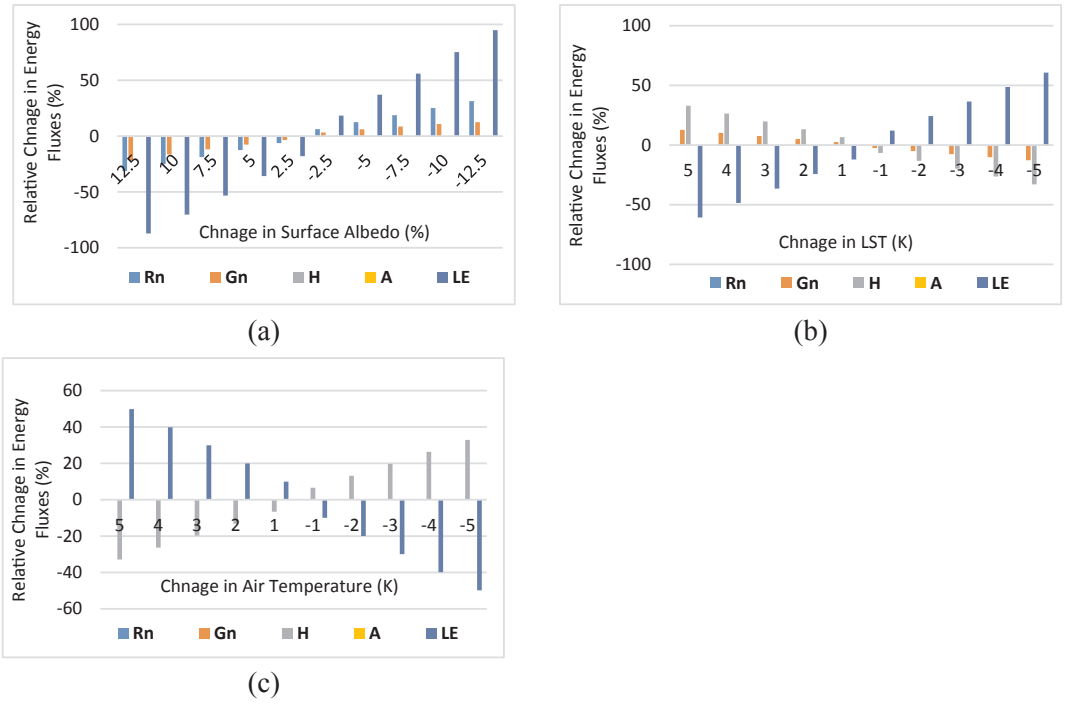

Fig. 8. Sensitivity of energy fluxes to changes of input parameters: (a) change in surface albedo, (b) change in LST, and (c) change in air temperature.

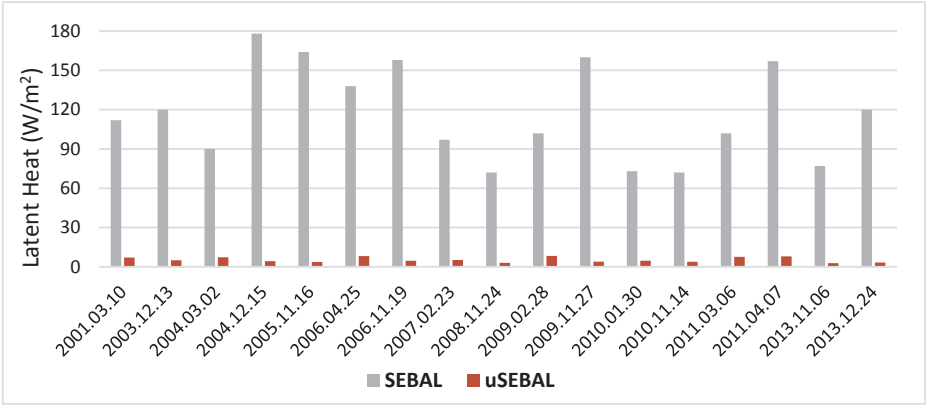

Fig. 9. Minimum observed latent heat (LE) in impervious urban areas.

a significant increase in air temperature tends to increase in ET in arid and semi-arid regions of Iran. The results of Yang et al. (2019) showed that potential ET is most sensitive to net radiation, followed by relative humidity, air temperature, wind speed, and soil heat flux in the Qilian Mountains, northwestern China. This study indicates the highest influence of solar radiation followed by air temperature. This finding is consistent with the study of Qiu et al., (2017), which identified that ET is strongly correlated with solar radiation in urban areas. DiGiovanni-White et al. (2018) also found the strongest influence of temperature and solar radiation on the determination of ET in a heterogeneous urban environment in New York City, (USA). In contrast, they noted the weak influence of wind speed and relative humidity on ET but underlined the importance of them as the variables varied the most amongst the sites. It should be noted that this study uses meteorological parameters from one weather station and lacks datasets from different locations. Urban environment is heterogeneous and results in strong variability in the micro-weather (DiGiovanni-White et al., 2018). This study acknowledges areas for future work in the evaluation of the influence of weather parameters on ET using datasets from multiple sites in an urban environment.

Model validation is important to estimate ET using RS data. This study uses pan evaporation and FAO Penman-Monteith based reference ET to evaluate the performance of the proposed approach. The model performance metrics indicate better performance of the uSEBAL than the SEBAL. It should be noted that the study site lacks an eddy flux tower, which limits the robustness of the validation of the modelled ET values thus, a sensitivity analysis is performed. The results of sensitivity analysis indicate that some of the energy budget components are highly sensitive to ET, which highlights the importance of its accurate estimation to reduce uncertainty. Considering the limitations of this study, we urge researchers to evaluate and validate the proposed approach in urban areas that have *in situ* measurements of surface energy fluxes over various land cover types. Moreover, future study is required to improve the uSEBAL by considering other parameters such as weather data of different locations, soil type, and moisture conditions.

5. Conclusions

ET is an important component of the hydrologic cycle. The hydrologic cycle starts with evaporation from the bodies of surface water and

transpiration from the vegetative land cover, and thus changes in land cover affect ET in urban areas where water and the evaporative surfaces are scarce. It is important to understand the spatial and temporal pattern of ET for managing urban landscapes and microclimates, and investigating urban water stress. Existing studies rarely estimate ET in a typical urban environment. This study proposes an approach to improve ET estimation for a heterogeneous urban environment based on the urban surface energy balance algorithm called the uSEBAL. The proposed approach shows the lowest ET for impervious urban areas, while the SEBAL shows the lowest ET for dry bare land, followed by impervious areas. The results indicate strong similarities in the maximum observed ET values between the models. However, there are deviations between the minimum and mean ET values. The model performance metrics show the satisfactory performance of the proposed approach to estimate ET in a heterogeneous urban environment. However, future study is required to test the transferability of the uSEBAL and to fully evaluate the applicability of this approach to other RS data. The results reported in this study confirm that the impervious areas are the dominant land cover in the urban areas where the human activities concentrate, and generate anthropogenic heat. Thus, this study supports the inclusion of this heat flux when estimating ET in a heterogeneous urban environment based on the surface energy balance algorithm. The sensitivity analysis indicates that variations in energy fluxes can affect ET and so care should be taken in the estimation of the model inputs. The proposed uSEBAL is of significance to understand water demand for diverse urban landscapes, and facilitate the monitoring of water stress in a heterogeneous urban environment.

CRediT authorship contribution statement

Mst Ilme Faridatul: Conceptualization, Methodology, Formal analysis Writing - original draft. **Bo Wu:** Supervision, Writing - review & editing. **Xiaolin Zhu:** Writing - review & editing. **Shuo Wang:** Writing - review & editing.

Declaration of Competing Interest

The authors declare that they have no known competing financial interests or personal relationships that could have appeared to influence the work reported in this paper.

Acknowledgments

The work described in this paper is supported by funding from the Hong Kong PhD Fellowship. The authors would like to thank the US Geological Survey (USGS) for making the Landsat datasets publicly available and the Bangladesh Meteorological Department (BMD) for providing the meteorological data.

Appendix A. Supplementary data

Supplementary data to this article can be found online at https://doi.org/10.1016/j.jhydrol.2019.124405.

References

Allen, R., Pruitt, W., 1991. FAO-24 reference evapotranspiration factors. J. Irrig. Drain. Eng. 117, 758–773.

Allen, R., Pereira, L.S., Raes, D., Smith, M., 1998. Crop evapotranspiration - Guidelines for computing crop water requirements – FAO Irrigation and drainage paper 56. Rome 300.

Allen, R., Tasumi, M., Trezza, R., 2007. Satellite-based energy balance for mapping evapotranspiration with internalized calibration (METRIC)-model. J. Irrig. Drain. Eng. 133, 380–394.

Bachour, R., Walker, W.R., Ticlavilca, A.M., Mckee, M., Maslova, I., 2014. Estimation of spatially distributed evapotranspiration using remote sensing and a relevance vector machine. J. Irrig. Drain. Eng. 140, 04014029-1–10.

Bastiaanssen, W.G.M., Menenti, M., Feddes, R.A., Holtslag, A.A.M., 1998. A remote sensing surface energy balance algorithm for land (SEBAL) 1. Formulation. *J. Hydrol.* 212, 198–212.

Bhattarai, N., Shaw, S.B., Quackenbush, L.J., Im, J., Niraula, R., 2016. Evaluating five remote sensing based single-source surface energy balance models for estimating daily evapotranspiration in a humid subtropical climate. Int. J. Appl. Earth Obs. Geoinf. 49, 75–86.

Chen, X., Chen, Y.D., Zhang, Z., 2007. A numerical modeling system of the hydrological cycle for estimation of water fluxes in the Huaihe River Plain Region, China. J. Hydrometeorol. 8, 702–714.

Chen, Y., Xia, J., Liang, S., Feng, J., Fisher, J.B., Li, X., Li, X., Liu, S., Ma, Z., Miyata, A., Mu, Q., Sun, L., Tang, J., Wang, K., Wen, J., Xue, Y., Yu, G., Zha, T., Zhang, L., Zhang, Q., Zhao, T., Zhao, L., Yuan, W., 2014. Comparison of satellite-based evapotranspiration models over terrestrial ecosystems in China. Remote Sens. Environ. 140, 279–293.

Cong, Z., Shen, Q., Zhou, L., Sun, T., Liu, J., 2017. Evapotranspiration estimation considering anthropogenic heat based on remote sensing in urban area. Sci. China Earth Sci. 60, 659–671.

DiGiovanni-White, K., Montalto, F., Gaffin, S., 2018. A comparative analysis of micrometeorological determinants of evapotranspiration rates within a heterogeneous urban environment. J. Hydrol. 562, 223–243.

Du, C., Yu, J., Wang, P., Zhang, Y., 2016. Reference evapotranspiration changes: sensitivities to and contributions of meteorological factors in the Heihe river basin of northwestern China (1961–2014). Adv. Meteorol. 2016, 1–17.

El Garouani, A., Boussema, M., Ennabli, H., 2000. Use of the geographic information system and remote sensing data for the estimation of real evapotranspiration at a regional scale. Int. J. Remote Sens. 21, 2811–2830.

El Tahir, M., Wenzhong, W., Xu, C.Y., Youjing, Z., Singh, V., 2012. Comparison of methods for estimation of regional actual evapotranspiration in data scarce regions: Blue Nile Region, Eastern Sudan. J. Hydrol. Eng. 17, 578–589.

Farah, H.O., Bastiaanssen, W.G.M., 2001. Impact of spatial variations of land surface parameters on regional evaporation: a case study with remote sensing data. Hydrol. Process. 15, 1585–1607.

Grimmond, C., Oke, T., 1991. An evapotranspiration-interception model for urban areas. Water Resour. Res. Washington, DC 27, 1739–1755.

Islam, M.S., Rahman, M.R., Shahabuddin, A., Ahmed, R., 2010. Changes in wetlands in Dhaka City: trends and physico-environmental consequences. J. Life Earth Sci. 5, 37–42.

Jassas, H., Kanoua, W., Merkel, B., 2015. Actual evapotranspiration in the Al-Khazir Gomal basin (Northern Iraq) using the surface energy balance algorithm for land (SEBAL) and water balance. Geosciences 5, 141–159.

Jensen, M., Burman, R., Allen, G., 1990. Evapotranspiration and irrigation water requirement ASCE manual and report on engineering practical , No.70, New York.

Jiang, L., Guli, J., Bao, A., Guo, H., Ndayisaba, F., 2017. Vegetation dynamics and responses to climate change and human activities in Central Asia. Sci. Total Environ. 599–600, 967–980.

Kato, S., Yamaguchi, Y., 2005. Analysis of urban heat-island effect using ASTER and ETM + Data: Separation of anthropogenic heat discharge and natural heat radiation from sensible heat flux. Remote Sens. Environ. 99, 44–54.

Kato, S., Yamaguchi, Y., 2007. Estimation of storage heat flux in an urban area using ASTER data. Remote Sens. Environ. 110, 1–17.

Kumar, V., Khan, S., Shaktibala, Rahul, A.K., 2018. Review of evapotranspiration methodologies. Am. J. Earth Sci. Eng. 1, 72–84.

Kustas, W.P., Norman, J.M., 1996. Use of remote sensing for evapotranspiration monitoring over land surfaces. Hydrol. Sci. J. 41, 495–516.

Li, S., Zhao, W., 2010. Satellite-based actual evapotranspiration estimation in the middle reach of the Heihe river basin using the SEBAL method. Hydrol. Process. 24, 3337–3344.

Liu, W., Hong, Y., Khan, S.I., Huang, M., Vieux, B., Caliskan, S., Groutb, T., 2010. Actual evapotranspiration estimation for different land use and land cover in urban regions using Landsat 5 data. J. Appl. Remote Sens. 4, 1–14.

Ma, W., Hafeez, M., Ishikawa, H., Ma, Y., 2013. Evaluation of SEBS for estimation of actual evapotranspiration using ASTER satellite data for irrigation areas of Australia. Theor. Appl. Climatol. 112, 609–616.

Magali, O.L., Isidro, C., Christopher, M.U.N., Samuel, O.F., Carlos, P.E., Claudio, B., Alfonso, C., 2016. Estimating evapotranspiration of an apple orchard using a remote sensing-based soil water balance. Remote Sens. 8, 253.

Makkink, G., 1957. Testing the Penman formula by means of Lysimeters. J. Inst. Water Eng. 11.

Mallick, J., Singh, C.K., Shashtri, S., Rahman, A., Mukherjee, S., 2012. Land surface emissivity retrieval based on moisture index from Landsat TM satellite data over heterogeneous surfaces of Delhi city. Int. J. Appl. Earth Obs. Geoinf. 19, 348–358.

Markham, B.L., Helder, D.L., 2012. Forty-year calibrated record of earth-reflected radiance from Landsat: a review. Remote Sens. Environ. 122, 30–40.

McVicar, T.R., Jupp, D.L.B., 1998. The current and potential operational uses of remote sensing to aid decisions on drought exceptional circumstances in Australia: a review. Agric. Syst. 57, 399–468.

McVicar, T.R., Roderick, M.L., Donohue, R.J., Li, L.T., Van Niel, T.G., Thomas, A., Grieser, J., Jhajharia, D., Himri, Y., Mahowald, N.M., Mescherskaya, A.V., Kruger, A.C., Rehman, S., Dinpashoh, Y., 2012. Global review and synthesis of trends in observed terrestrial near-surface wind speeds: Implications for evaporation. J. Hydrol. 416–417, 182–205.

Minacapilli, M., Agnese, C., Blanda, F., Cammalleri, C., Ciraolo, G., Urso, G., Iovino, M., Pumo, D., Provenzano, G., Rallo, G., 2009. Estimation of actual evapotranspiration of Mediterranean perennial crops by means of remote-sensing based surface energy balance models. Hydrol. Earth Syst. Sci. 13, 1061.

Mutiga, J.K., Su, Z., Woldai, T., 2010. Using satellite remote sensing to assess

evapotranspiration: case study of the upper Ewaso Ng'iro North Basin, Kenya. Int. J. Appl. Earth Observ. Geoinf. 12, S100–S108.
Nouri, H., Beecham, S., Kazemi, F., Hassanli, A.M., 2012. A review of ET measurement techniques for estimating the water requirements of urban landscape vegetation. Urban Water J. 10, 1–13.
Oberg, J.W., Melesss, A.M., 2006. Evapotranspiration dynamics at an ecohydrological restoration site: an energy balance and remote sensing approach 1. J. Am. Water Resour. Assoc. 42, 565–582.
Oke, T.R., 1979. Boundary layer climates. Weather 34, 370.
Oke, T.R., 1982. The energetic basis of the urban heat island. Q. J. R. Meteorolog. Soc. 108, 1–24.
Priestley, C.H.B., Taylor, R.J., 1972. On the assessment of surface heat flux and evaporation using large-scale parameters. Mon. Weather Rev. 100, 81–92.
Qiu, G., Tan, S., Wang, Y., Yu, X., Yan, C., 2017. Characteristics of evapotranspiration of urban lawns in a sub-tropical megacity and its measurement by the 'Three Temperature Model + Infrared Remote Sensing' method. Remote Sens. 9, 502.
Rahman, M.A., Wiegand, B.A., Badruzzaman, A.B.M., Ptak, T., 2013. Hydrogeological analysis of the upper Dupi Tila Aquifer, towards the implementation of a managed aquifer-recharge project in Dhaka City, Bangladesh. Hydrogeol. J. 21, 1071–1089.
Roerink, G.J., Su, Z., Menenti, M., 2000. S-SEBI: a simple remote sensing algorithm to estimate the surface energy balance. Phys. Chem. Earth Part B 25, 147–157.
Rwasoka, D.T., Gumindoga, W., Gwenzi, J., 2011. Estimation of actual evapotranspiration using the Surface Energy Balance System (SEBS) algorithm in the Upper Manyame catchment in Zimbabwe. Phys. Chem. Earth. 36, 736–746.
Scanlon, B., Healy, R., Cook, P., 2002. Choosing appropriate techniques for quantifying groundwater recharge. Hydrogeol. J. 10, 18–39.
Senay, G.B., Bohms, S., Singh, R.K., Gowda, P.H., Velpuri, N.M., Alemu, H., Verdin, J.P., 2013. Operational evapotranspiration mapping using remote sensing and weather datasets: a new parameterization for the SSEB approach. J. Am. Water Resour. Assoc. 49, 577–591.
Shi, H.Y., Li, T.J., Wang, G.Q., 2017. Temporal and spatial variations of potential evaporation and the driving mechanism over Tibet during 1961–2001. Hydrol. Sci. J. 62 (9), 1469–1482.
Su, Z., 2002. The surface energy balance system (SEBS) for estimation of turbulent heat fluxes. Hydrol. Earth Syst. Sci. 6, 85–99.
Sun, Z., Wei, B., Su, W., Shen, W., Wang, C., You, D., Liu, Z., 2011. Evapotranspiration estimation based on the SEBAL model in the Nansi Lake Wetland of China. Math. Comput. Modell. 54, 1086–1092.
Tabari, H., Aeini, A., Talaee, P.H., Some, E.B.S., 2012. Spatial distribution and temporal variation of reference evapotranspiration in arid and semi-arid regions of Iran. Hydrol. Process. 26, 500–512.
Timmermans, W.J., Kustas, W.P., Anderson, M.C., French, A.N., 2007. An intercomparison of the surface energy balance algorithm for land (SEBAL) and the two-source energy balance (TSEB) modeling schemes. Remote Sens. Environ. 108, 369–384.
Tomer, M.D., Schilling, K.E., 2009. A simple approach to distinguish land-use and climate-change effects on watershed hydrology. J. Hydrol. 376, 24–33.
Trout, K., Ross, M. Estimating evapotranspiration in urban environments. In: Tellam, J.H., Rivett, M.O., Israfilov, R.G., Herringshaw, L.G., eds. Urban groundwater management and sustainability, 2006 Dordrecht. Springer Netherlands, 157–168.
Van De Griend, A.A., Owe, M., 1993. On the relationship between thermal emissivity and the normalized difference vegetation index for natural surfaces. Int. J. Remote Sens. 14, 1119–1131.
Verma, S., 1989. Aerodynamic resistances to transfers of heat, mass and momentum. Estimation Areal Evapotranspiration 177, 13–20.
Wagle, P., Bhattarai, N., Gowda, P.H., Kakani, V.G., 2017. Performance of five surface energy balance models for estimating daily evapotranspiration in high biomass sorghum. ISPRS J. Photogramm. Remote Sens. 128, 192–203.
Wang, K., Dickinson, R.E., 2012. A review of global terrestrial evapotranspiration: observation, modeling, climatology, and climatic variability. Rev. Geophys. 50, 1–54.
Wang, C., Yang, J., Myint, S.W., Wang, Z.H., Tong, B., 2016. Empirical modeling and spatio-temporal patterns of urban evapotranspiration for the Phoenix metropolitan area, Arizona. GIScience Remote Sens. 53, 778–792.
Waters, R., Allen, R., Tasumi, M., Trezza, R., Bastiaanssen, W., 2002. SEBAL surface energy balance algorithms, Advanced training and users manual, Version 1.0. The Idaho Department of Water Resources, USA.
Weng, Q., Hu, X., Quattrochi, D.A., Liu, H., 2014. Assessing intra-urban surface energy fluxes using remotely sensed ASTER imagery and routine meteorological data: a case study in Indianapolis, U.S.A. I*EEE J. Sel. Top. Appl. Earth Obs. Remote Sens.* 7, 4046–4057.
Wong, M.S., Yang, J., Nichol, J., Weng, Q., Menenti, M., Chan, P.W., 2015. Modeling of anthropogenic heat flux using HJ-1B Chinese small satellite image: a study of heterogeneous urbanized areas in Hong Kong. Geosci. Remote Sens. Lett. IEEE 12, 1466–1470.
Wu, H., 2016. Evapotranspiration estimation of Platycladus Orientalis in Northern China based on various models. J. For. Res. 27, 871–878.
Wulder, M.A., White, J.C., Loveland, T.R., Woodcock, C.E., Belward, A.S., Cohen, W.B., Fosnight, E.A., Shaw, J., Masek, J.G., Roy, D.P., 2016. The global Landsat archive: status, consolidation, and direction. Remote Sens. Environ. 185, 271–283.
Xiong, J., Wu, B., Yan, N., Zeng, Y., Liu, S., 2010. Estimation and validation of land surface evaporation using remote sensing and meteorological data in North China. IEEE J. Sel. Top. Appl. Earth Obs. Remote Sens. 3, 337–344.
Yang, Y., Chen, R., Song, Y., Han, C., Liu, J., Liu, Z., 2019. Sensitivity of potential evapotranspiration to meteorological factors and their elevational gradients in the Qilian Mountains, Northwestern China. J. Hydrol. 568, 147–159.
Zhang, K., Kimball, J.S., Running, S.W., 2016. A review of remote sensing based actual evapotranspiration estimation. Wiley Interdiscip. Rev.: Water 3, 834–853.